2-1-2008

Low Complexity Soft-Input Soft-Output Block Decision Feedback Equalization

Jingxian Wu

Y. Rosa Zheng
Missouri University of Science and Technology, zhengyr@mst.edu

Recommended Citation

J. Wu and Y. R. Zheng, "Low Complexity Soft-Input Soft-Output Block Decision Feedback Equalization," *IEEE Journal on Selected Areas in Communications*, Institute of Electrical and Electronics Engineers (IEEE), Feb 2008.
The definitive version is available at https://doi.org/10.1109/JSAC.2008.080205

Low Complexity Soft-Input Soft-Output Block Decision Feedback Equalization

Jingxian Wu, *Member, IEEE,* and Yahong R. Zheng, *Senior Member, IEEE,*

***Abstract*—A low complexity soft-input soft-output (SISO) block decision feedback equalizer (BDFE) is presented for turbo equalization. The proposed method employs a sub-optimum sequence-based detection, where the soft-output of the equalizer is calculated by evaluating an approximation of the sequence-based *a posteriori* probability (APP) of the data symbol. The sequence-based APP approximation is enabled by the adoption of both soft *a priori* information and soft decision feedback, and it leads to better performance and faster convergence compared to symbol-based detection methods as used by most other low complexity equalizers. The performance and convergence property of the proposed algorithm is analyzed by using extrinsic information transfer (EXIT) chart. Both analytical and simulation results show that the new equalizer can achieve a performance similar to that of trellis-based equalization algorithms, with a complexity similar to linear SISO minimum mean square error equalizers.**

***Index Terms*—Turbo equalization, sequence-based detection, BDFE, soft decision feedback, EXIT.**

I. Introduction

TURBO equalization is a joint equalization and decoding scheme used in communication systems with coded data transmitted over inter-symbol interference (ISI) channel [1], [2]. Turbo equalizers achieve performance improvement over conventional equalizers and decoders by iteratively exchanging soft extrinsic information between a soft-input soft-output (SISO) equalizer and a SISO decoder. Trellis-based soft decoding algorithms, such as Bahl-Cocke-Jelinek-Raviv (BCJR) algorithm [3], or soft output Viterbi algorithm (SOVA) [1], [4], are usually employed in SISO equalizer/decoder to maximize the sequence-based symbol *a posteriori* probability (APP). For systems with high modulation levels and/or long channel length, the trellis-based SISO equalizers become prohibitively complex. Therefore, the design of low complexity SISO turbo equalizers has attracted considerable interests recently [5] – [14]. Current approaches to low complexity algorithms can be roughly classified into three categories.

First, reducing the number of states in the trellis structure of an ISI channel leads to sub-optimum trellis-based equalizers [5], [6]. In [5], the BCJR algorithm is performed over a reduced state trellis, which is formulated by considering only dominant taps of the equivalent channel. ISI introduced by non-dominant channel taps are canceled by hard decisions [5], or soft decisions [6], from previous iterations. The complexity of such equalizers grows exponentially with the number of dominant channel taps.

Second, linear minimum mean square error (MMSE) based SISO equalization algorithms [7] – [12] provide a reasonable trade-off between complexity and performance. The MMSE equalizers treat the data symbols as random variables with mean and variance computed from the *a priori* information. Complexity reduction in linear SISO MMSE algorithms is mainly due to symbol-by-symbol detection, *i.e.*, the APP of each symbol is calculated individually based on a Gaussian assumption of the MMSE filter output.

Third, non-linear SISO equalizers are designed by employing tentative hard decisions from the same iteration [13], or previous iteration [14], for ISI cancellation. To reduce error propagation arising from tentative hard decisions, a soft decision feedback equalizer is proposed in [15], which employs the *a posteriori* mean of the data symbols for ISI cancellation. Similar to linear SISO equalizers, symbol-based detection is used in the existing non-linear equalizers.

Motivated by the respective advantages and limitations of the methods in the literature, we develop a new, non-linear, sub-optimum sequence-based block decision feedback equalizer (BDFE). Many of the performance enhancing features from the existing methods are used as building blocks of the new algorithm. The BDFE filters are dynamically formulated with the help of the *a priori* mean and variance of the data symbols as in [7]-[12]; the decision feedback is used for ISI cancellation as in [13]-[16]; specifically, the soft decision feedback is employed to reduce error propagation as in [15].

The main contribution of the proposed method is the employment of a sub-optimum sequence-based detection. In the proposed equalizer, the APP of each data symbol is calculated by collecting information from all related samples at the receiver, whereas no trellis structure is used. The sequence-based detection is made possible by utilizing soft decisions from both current iteration and previous iteration, and it improves over the symbol-by-symbol processing adopted by most existing methods. The non-linearity of the proposed method arises from decision feedback as well as the sub-optimum sequence-based detection. The combination of the sequence-based detection, along with those proven effective equalizer features, result in an equalizer with better performance and faster convergence rate.

The performance of the proposed algorithm is analyzed by using the extrinsic information transfer (EXIT) chart [18], [19]. Both analytical results and simulation results show that the proposed algorithm can achieve a performance similar

Manuscript received March 31, 2007; revised November 1, 2007. Part of this paper was previously presented at the 2007 IEEE Global Telecommunication Conference (Globecom'07), Washington D.C., USA.

J. Wu is with the Department of Engineering Science, Sonoma State University, Rohnert Park, CA 94928, USA (e-mail: jingxian.wu@sonoma.edu).

Y. R. Zheng is with the Department of Electrical and Computer Engineering, Missouri University of Science & Technology (former University of Missouri), Rolla, MO 65409 USA (e-mail: zhengyr@mst.edu).

Digital Object Identifier 10.1109/JSAC.2008.080205.

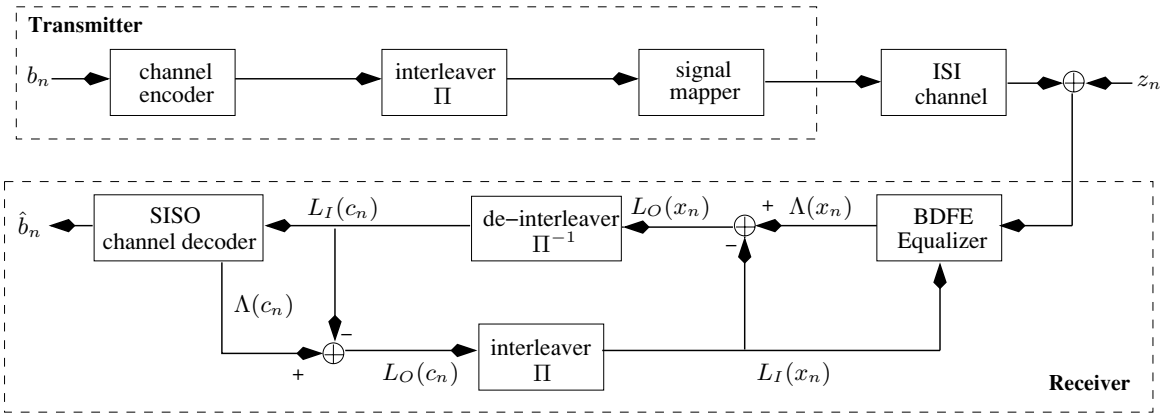

Fig. 1. Block diagram of a communication system with turbo equalization.

to that of trellis-based algorithms, with a complexity on the same order as linear MMSE equalizers. In addition, the new algorithm converges at a rate much faster compared to other equalization algorithms, and this will further reduce the overall complexity of the system due to the reduction of the number of iterations.

The remainder of this papers is organized as follows. System model with a brief introduction of turbo principle is presented in Section II. The new SISO BDFE algorithm with sequence-based detection is developed in Section III. The performance of the proposed algorithms is analyzed in Section IV with the tool of EXIT chart. Bit error rate (BER) results obtained from simulations under practical system configurations are given in Section V, and Section VI concludes the paper.

II. System Model

The block diagram of a communication system employing turbo equalization is shown in Fig. 1. At the communication transmitter, the binary information, $b_n \in \{-1, +1\}$, is passed through a convolutional encoder followed by an interleaver, and no trellis termination is used in the convolutional encoder. The output of the interleaver is divided into blocks with length $K \cdot N$, where $K = \log_2 M$, M is the modulation level, and N is the number of modulated symbols per block. The output of the interleaver can be denoted in vector form as $\mathbf{x} = [\mathbf{x}_1, \mathbf{x}_2, \cdots, \mathbf{x}_N]^T \in \mathcal{B}^{KN\times 1}$, where $\mathbf{x}_n = [x_1, \cdots, x_K] \in \mathcal{B}^{1\times K}$, and $\mathbf{A}^T$ is the transpose of matrix $\mathbf{A}$. The modulator maps K-bit data, $\mathbf{x}_n$, to one modulation symbol, $s_n \in \mathcal{S}$, where $\mathcal{S}$ is the modulation constellation set with cardinality M.

The modulated data symbols are distorted by the ISI channel and additive white Gaussian noise (AWGN). The discrete-time representation of the communication system is

$$y_n = \sum_{l=0}^{L-1} h_l s_{n-l} + z_n, \text{ for } n = 1, 2, \cdots, N. \tag{1}$$

where y_n is the symbol-spaced sample at the output of the receive filter, z_n is the zero-mean AWGN sample, and h_l is the equivalent discrete-time composite channel impulse response resulted from the cascade of transmit filter, ISI channel, and receive filter [17]. The system model described in (1) can be represented in matrix format as

$$\mathbf{y} = \mathbf{H}\mathbf{s} + \mathbf{z}, \tag{2}$$

where $\mathbf{y} = [y_1, \cdots, y_N]^T \in \mathcal{C}^{N\times 1}$, $\mathbf{s} = [s_1, \cdots, s_N]^T \in \mathcal{C}^{N\times 1}$, and $\mathbf{z} = [z_1, \cdots, z_N]^T \in \mathcal{C}^{N\times 1}$ are the receive sample vector, modulation symbol vector, and noise vector, respectively, and the channel matrix $\mathbf{H}$ is defined by

$$\mathbf{H} = \begin{pmatrix} h_0 & 0 & 0 & \cdots & \cdots & 0 \\ \vdots & \ddots & & \ddots & & \vdots \\ 0 & h_{L-1} & \cdots & h_0 & \cdots & 0 \\ \vdots & & \ddots & & \ddots & \vdots \\ 0 & \cdots & 0 & h_{L-1} & \cdots & h_0 \end{pmatrix} \in \mathcal{C}^{N\times N}. \tag{3}$$

The system equation of (2) and the channel matrix defined in (3) indicate that there is no inter-block interference (IBI). The IBI-free communication is achieved by using a short guard interval between blocks. Either zeros or known pilot symbols with length L can be transmitted during the guard interval. The guard interval results in a rate loss of $L/(N+L) \times 100\%$.

Turbo equalizer consists of a SISO equalizer and a SISO convolutional decoder, which are separated by an interleaver, $\Pi(\cdot)$, and a de-interleaver, $\Pi^{-1}(\cdot)$. During each iteration, the SISO equalizer calculates the *a posteriori* log likelihood ratio (LLR) for each code bit x_n as

$$\Lambda(x_n|\mathbf{y}) = \ln \frac{P(x_n = +1|\mathbf{y})}{P(x_n = -1|\mathbf{y})}. \tag{4}$$

Using Bayes' Rule, we can write (4) as

$$\Lambda(x_n|\mathbf{y}) = \underbrace{\ln \frac{\sum_{\forall \mathbf{x}: x_n=+1} P(\mathbf{y}|\mathbf{x}) \prod_{n'\neq n} P(x_{n'})}{\sum_{\forall \mathbf{x}: x_n=-1} P(\mathbf{y}|\mathbf{x}) \prod_{n'\neq n} P(x_{n'})}}_{L_O(x_n)} + L_I(x_n)$$

where $L_I(x_n) \triangleq \ln \frac{P(x_n=+1)}{P(x_n=-1)}$ is the *a priori* information of bit x_n, and it is obtained by interleaving the soft-output of the convolutional decoder from the previous iteration. The *a priori* information is assumed to be independent with each other. In the first iteration, there is no *a priori* information available and we have $L_I(x_n) = 0, \forall n$.

The extrinsic LLR, $L_O(x_n) = \Lambda(x_n|\mathbf{y}) - L_I(x_n)$, will be de-interleaved to $L_I(c_n) = \Pi^{-1}(L_O(x_n))$, which is used as

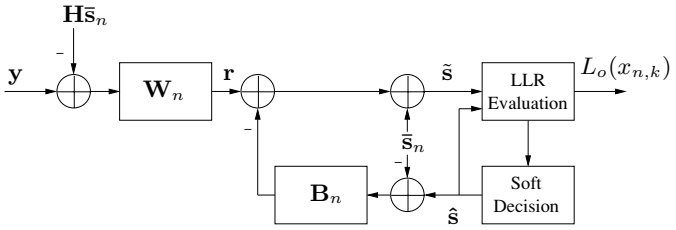

Fig. 2. SISO block decision feedback equalizer.

the *a priori* information, or, soft-input, of the convolutional decoder. The convolutional decoder calculates the extrinsic LLR for each code bit by exploiting the code trellis structure as well as the *a priori* information $L_I(c_n)$. The extrinsic LLR for the code bit c_n can be expressed as

$$L_O(c_n)=\ln \frac{P(c_n=+1|L_I(c_1),\cdots,L_I(c_{N_c}))}{P(c_n=-1|L_I(c_1),\cdots,L_I(c_{N_c}))} - \underbrace{\ln \frac{P(c_n=+1)}{P(c_n=-1)}}_{L_I(c_n)},$$

where $N_c = N/R$ is the number of code bits in each block, with R being the code rate, and N the number of bits per block.

The extrinsic LLR at the output of the convolutional decoder is interleaved as $L_I(x_n) = \Pi\left(L_O(c_n)\right)$, which is fed back to the equalizer as the *a priori* information for the next iteration. At the final iteration, the SISO convolutional decoder estimates the original binary information, $b_n \in \{-1, 1\}$, as

$$\hat{b}_n = \underset{b_n\in\{-1,1\}}{\operatorname{argmax}} P\left(b_n|L_I(c_1)+L_O(c_1),\cdots,L_I(c_{N_c})+L_O(c_{N_C})\right).$$

The statistically independent *a priori* LLRs $L_O(x_n)$ and $L_O(c_n)$ are fed back to each other iteratively and lead to improvement in BER performance. This essential feature achieves the turbo principle. In both the equalizer and convolutional decoder, the exact *a posteriori* LLR can be calculated by using the BCJR algorithm or SOVA algorithm, which can effectively exploit the trellis structure of the ISI channel and convolutional code. However, the complexity of the trellis-based equalizers increases exponentially with the modulation level M and channel length L. The computational complexity makes it prohibitively expensive to implement the trellis-based BCJR or SOVA algorithm in the equalizer.

III. Turbo Equalization Using SISO MMSE-BDFE

In this section, a SISO minimum mean square error based block decision feedback equalizer (MMSE-BDFE) is proposed for low complexity turbo equalization.

A. Development of SISO MMSE-BDFE

MMSE-BDFE algorithm was originally developed in [16] for hard-input hard-output equalization. In [16], the data symbols are assumed to be zero mean since no statistical data information is available at the input of the equalizer. With soft *a priori* information, a SISO MMSE-BDFE algorithm with non-zero mean data vectors and statistical filters are derived in this subsection. The block diagram of the SISO MMSE-BDFE is shown in Fig. 2.

The operation of the SISO MMSE-BDFE requires the *a priori* mean vector, $\bar{\mathbf{s}} = \mathbb{E}[\mathbf{s}]$, and the *a priori* covariance matrix, $\mathbf{\Phi} = \mathbb{E}\left[\mathbf{s}\mathbf{s}^H\right]$, of the data symbols, where $\mathbb{E}$ denotes mathematical expectation. The values of $\bar{\mathbf{s}}$ and $\mathbf{\Phi}$ can be calculated from the bit *a priori* LLR as [9]

$$\begin{aligned} \bar{s}_n &= \sum_{m=1}^{M} \chi_m P(s_n = \chi_m), \\ \sigma^2_{s_n} &= \sum_{m=1}^{M} (\chi_m - \bar{s}_n)^2 P(s_n = \chi_m). \end{aligned} \tag{5}$$

where $\chi_m \in \mathcal{S}$ is an M-ary modulated symbol mapped to the binary vector $\mathbf{b} = [b_1, \cdots, b_K]$, $P(s_n = \chi_m) = \prod_{k=1}^{K} P(x_{n,k} = b_k)$ is the symbol *a priori* probability, and $P(x_{n,k} = b_k)$ is the bit *a priori* probability that can be derived from the bit *a priori* LLR, $L_I(x_n)$, as

$$P(x_n = -1) = \left[1 + e^{L_I(x_n)}\right]^{-1}, \tag{6a}$$

$$P(x_n = +1) = 1 - P(x_n = -1). \tag{6b}$$

The modulated information symbols, s_n, for $n = 1, \cdots, N$, can be assumed to be independent due to the bit interleaving performed before modulation. Therefore, the covariance matrix, $\mathbf{\Phi}$, is a diagonal matrix with $\sigma^2_{s_n}$ on its diagonal.

To avoid instability caused by positive feedback during the iterative operation, the *a priori* information of symbol s_n should not be used during the detection of s_n itself. For this reason, during the equalization of s_n, define the *a priori* mean vector, $\bar{\mathbf{s}}_n$, and *a priori* covariance matrix, $\mathbf{\Phi}_n$, as

$$\begin{aligned} \bar{\mathbf{s}}_n &= [\bar{s}_1, \cdots, \bar{s}_{n-1}, 0, \bar{s}_{n+1}, \cdots, \bar{s}_N]^T, \\ \mathbf{\Phi}_n &= \operatorname{diag}[\sigma^2_{s_1}, \cdots, \sigma^2_{s_{n-1}}, 1, \sigma^2_{s_{n+1}}, \cdots, \sigma^2_{s_N}]. \end{aligned} \tag{7}$$

In the definition, the mean and variance of s_n, which is the symbol to be detected, are assumed to be 0 and 1, respectively [9].

The MMSE-BDFE performs detection of the nth symbol, s_n, through two block filters: a feedforward filter, $\mathbf{W}_n \in \mathcal{C}^{N\times N}$, and a zero diagonal feedback filter, $\mathbf{B}_n \in \mathcal{C}^{N\times N}$. From Fig. 2, the decision vector before LLR calculation can be written as

$$\tilde{\mathbf{s}} = \mathbf{W}_n[\mathbf{y} - \mathbf{H}\bar{\mathbf{s}}_n] - \mathbf{B}_n[\hat{\mathbf{s}} - \bar{\mathbf{s}}_n] + \bar{\mathbf{s}}_n, \tag{8}$$

where $\bar{\mathbf{s}}_n$ is the *a priori* mean vector of $\mathbf{s}$ as defined in (7). The vector, $\hat{\mathbf{s}} = [\hat{s}_1, \hat{s}_2, \cdots, \hat{s}_N]^T \in \mathcal{C}^{N\times 1}$, contains tentative soft decisions from both current iteration and previous iteration. The soft decision is defined as the *a posteriori* mean of the symbol [15], and it can be calculated as

$$\hat{s}_n = \sum_{m=1}^{M} P\left(s_n = \chi_m|\mathbf{y}\right)\chi_m, \tag{9}$$

where $\chi_m \in \mathcal{S}$ is the modulation symbol, and $P\left(s_n = \chi_m|\mathbf{y}\right)$ is the APP at the output of the equalizer. The adoption of *a posteriori* mean based soft decision will reduce the effects of error propagation, thus leading to better system performance.

The BDFE filters, $\mathbf{W}_n$ and $\mathbf{B}_n$, are derived by following the MMSE criterion. With the common assumption of perfect

decision feedback, *i.e.*, $\hat{\mathbf{s}} = \mathbf{s}$, the error vector of BDFE can be written as

$$\mathbf{e}_n = \mathbf{W}_n(\mathbf{y} - \mathbf{H}\bar{\mathbf{s}}_n) - (\mathbf{B}_n + \mathbf{I}_N)(\mathbf{s} - \bar{\mathbf{s}}_n). \quad (10)$$

where $\mathbf{I}_N$ is an $N \times N$ identity matrix. The orthogonality principle, $E\left[\mathbf{e}_n(\mathbf{y} - \mathbf{H}\bar{\mathbf{s}}_n)^H\right] = 0$, is used to minimize the mean square error, $E\left[\|\mathbf{e}_n\|^2\right] = E\left[\mathbf{e}_n^H\mathbf{e}_n\right]$, with the expectation operation performed over both the data symbols and noise, and the result is [16]

$$\mathbf{W}_n = \mathbf{G}_n\mathbf{\Phi}_n\mathbf{H}^H(\mathbf{H}\mathbf{\Phi}_n\mathbf{H}^H + N_0\mathbf{I}_N)^{-1}. \quad (11)$$

where $\mathbf{G}_n = \mathbf{B}_n + \mathbf{I}_N$, $\mathbf{\Phi}_n$ is the *a priori* covariance matrix as defined in (7), and N_0 is the AWGN variance.

Combining (10) and (11), we have the error vector as $\mathbf{e}_n = \mathbf{G}_n\epsilon_n$, with

$$\epsilon_n = \mathbf{\Phi}_n\mathbf{H}^H(\mathbf{H}\mathbf{\Phi}_n\mathbf{H}^H + N_0\mathbf{I}_N)^{-1}(\mathbf{y} - \mathbf{H}\bar{\mathbf{s}}) - (\mathbf{s} - \bar{\mathbf{s}}) \quad (12)$$

being the error vector of a linear MMSE equalizer. The covariance matrix, $\mathbf{\Phi}_{\epsilon\epsilon} = E[\epsilon_n\epsilon_n^H]$, is

$$\begin{aligned}\mathbf{\Phi}_{\epsilon\epsilon} &= \mathbf{\Phi}_n - \mathbf{\Phi}_n\mathbf{H}^H\left(\mathbf{H}\mathbf{\Phi}_n\mathbf{H}^H + N_0\mathbf{I}_N\right)^{-1}\mathbf{H}\mathbf{\Phi}_n, \\ &= \left(\mathbf{\Phi}_n^{-1} + \frac{1}{N_0}\mathbf{H}^H\mathbf{H}\right)^{-1}, \end{aligned} \quad (13)$$

where the identity, $\mathbf{A}^{-1} + \mathbf{A}^{-1}\mathbf{C}(\mathbf{G} - \mathbf{D}\mathbf{A}^{-1}\mathbf{C})^{-1}\mathbf{D}\mathbf{A}^{-1} = (\mathbf{A} - \mathbf{C}\mathbf{G}^{-1}\mathbf{D})^{-1}$, is used in the above equation. It should be noted that the inverse of the *a priori* covariance matrix, $\mathbf{\Phi}_n$, is used in (13). Since the uncertainty of each symbol decreases with the evolution of iterations, the *a priori* symbol variances, which are on the diagonal of $\mathbf{\Phi}_n$, might tend to zero after several iterations. To avoid numerical instability caused by the inverse of zero, a small threshold value, *e.g.*, $\sigma_0^2 = 10^{-5}$, is used to replace the diagonal elements of $\mathbf{\Phi}_n$ with values less than σ_0^2. This approximation doesn't apparently affect the performance of the system due to the fact that, the matrix $\mathbf{\Phi}_{\epsilon\epsilon}$ depends on the *inverse* of $\mathbf{\Phi}_n^{-1} + \frac{1}{N_0}\mathbf{H}^H\mathbf{H}$. Therefore, a small enough σ_0 will lead to an approximation error that is acceptable under certain numerical precision limits.

From (13), the covariance matrix $\mathbf{\Phi}_{ee} = E[\mathbf{e}_n\mathbf{e}_n^H]$ can be expressed by

$$\mathbf{\Phi}_{ee} = \mathbf{G}_n\left(\mathbf{\Phi}_n^{-1} + \frac{1}{N_0}\mathbf{H}^H\mathbf{H}\right)^{-1}\mathbf{G}_n^H. \quad (14)$$

Since $E(\|\mathbf{e}_n\|^2) = \text{trace}\,(\mathbf{\Phi}_{ee})$, the solution of the MMSE problem is equivalent to find unit diagonal matrix $\mathbf{G}_n = \mathbf{B}_n + \mathbf{I}_N$ such that trace $(\mathbf{\Phi}_{ee})$ is minimized. In addition, suboptimum decision feedback equalization requires the matrix $\mathbf{G}_n$ be in its minimum phase form, *i.e.*, the power of the matrix is concentrated on elements close to the main diagonal. The solution satisfying the above conditions can be obtained from the Cholesky decomposition of $\mathbf{\Phi}_n^{-1} + \frac{1}{N_0}\mathbf{H}^H\mathbf{H}$ as [16]

$$\mathbf{\Phi}_n^{-1} + \frac{1}{N_0}\mathbf{H}^H\mathbf{H} = \mathbf{L}_n^H\mathbf{L}_n, \quad (15)$$

where $\mathbf{L}_n$ is an upper triangular matrix. Normalizing $\mathbf{L}_n$ with respect to its main diagonal leads to

$$\mathbf{L}_n^H\mathbf{L}_n = \mathbf{U}_n^H\mathbf{D}_n\mathbf{U}_n \quad (16)$$

where $\mathbf{U}_n \in \mathcal{C}^{N\times N}$ is an upper triangular matrix with unit diagonal elements, $\mathbf{D}_n \in \mathcal{R}^{N\times N}$ is a diagonal matrix, and $\mathbf{L}_n = \sqrt{\mathbf{D}_n}\mathbf{U}_n$. With the Cholesky decomposition described in (15), the feedforward matrix, $\mathbf{W}_n$, and feedback matrix, $\mathbf{B}_n$, are

$$\begin{aligned}\mathbf{B}_n &= \mathbf{U}_n - \mathbf{I}_N, \\ \mathbf{W}_n &= \mathbf{U}_n\mathbf{\Phi}_n\mathbf{H}^H\left(\mathbf{H}\mathbf{\Phi}_n\mathbf{H}^H + N_0\mathbf{I}_N\right)^{-1}. \end{aligned} \quad (17)$$

It should be noted that Cholesky decomposition was also adopted in [12] for a linear extending window MMSE method. The Cholesky decomposition in [12] was used to assist the recursive calculation of matrix inversion, and its function is quite different from the Cholesky decomposition used in this paper.

With the filters given in (17), the wireless communication system described in (2) is converted to an equivalent system as (c.f. (10))

$$\mathbf{r} = \mathbf{W}_n(\mathbf{y} - \mathbf{H}\bar{\mathbf{s}}_n) = \mathbf{G}_n(\mathbf{s} - \bar{\mathbf{s}}_n) + \mathbf{e}_n, \quad (18)$$

where $\mathbf{r} = [r_1, r_2, \cdots, r_N]^T$ and $\mathbf{e}_n$ are the receive sample vector and noise sample vector of the equivalent system, respectively, and $\mathbf{G}_n = \mathbf{B}_n + \mathbf{I}_N$ is the equivalent channel matrix. The covariance matrix of the equivalent noise component is $\mathbf{\Phi}_{ee} = \mathbf{D}_n^{-1}$. Since $\mathbf{D}_n$ is diagonal, the noise components are uncorrelated.

B. Sequence-based A Posteriori Probability Evaluation

The calculation of the soft output of the equalizer is described in this subsection. The equivalent system described in (18) enables a sequence-based detection, *i.e.*, one symbol, s_n, can be detected by collecting information of the entire data block, $\mathbf{r} = \mathbf{W}_n(\mathbf{y} - \mathbf{H}\bar{\mathbf{s}}_n)$. This is different from the classical decision feedback equalizers, *e.g.*, [15], [16], where each data symbol is detected by using only the current equalizer output.

From (18), define the sequence-based symbol APP, $P\left(s_n^{(i)}|\mathbf{r}\right)$, of the ith iteration as

$$P\left(s_n^{(i)}|\mathbf{r}\right) = \frac{P(\mathbf{r}|s_n)P(s_n)}{p(\mathbf{r})}, \quad (19)$$

Since the sample sequence $\mathbf{r}$ depends on $[s_1, \cdots, s_N]$, the likelihood function, $P(\mathbf{r}|s_n)$, can be expressed as

$$P(\mathbf{r}|s_n) = P\left(\mathbf{r}|\hat{\mathbf{s}}_n^{(i)}\right), \quad (20)$$

where $\hat{\mathbf{s}}_n^{(i)} = [s_n, \hat{s}_1^{(i-1)}, \cdots, \hat{s}_{n-1}^{(i-1)}, \hat{s}_{n+1}^{(i)}, \cdots, \hat{s}_N^{(i)}]$, with $[\hat{s}_{n+1}^{(i)}, \cdots, \hat{s}_N^{(i)}]$ being soft decisions from the current iteration, and $[\hat{s}_1^{(i-1)}, \cdots, \hat{s}_{n-1}^{(i-1)}]$ soft decisions from the previous iteration. The equation holds since all the soft decisions are deterministic.

In the equivalent system representation given in (18), the noise samples are uncorrelated with a diagonal covariance matrix $\mathbf{\Phi}_{ee} = \mathbf{D}_n^{-1}$. Based on the assumption that the equivalent noise vector, $\mathbf{e}_n$, is Gaussian distributed, the likelihood function, $P\left(\mathbf{r}|\hat{\mathbf{s}}_n^{(i)}\right)$, can be approximated as

$$p\left(\mathbf{r}|\hat{\mathbf{s}}_n^{(i)}\right) \approx \prod_{k=1}^{N}\frac{1}{\pi\sigma_k}\exp\left\{-\frac{|\rho_{n,k}(s_n)|^2}{\sigma_k^2}\right\}, \quad (21)$$

$$\rho_{n,k}(s_n) = \begin{cases} r_k - \sum_{l=k}^{N} g_{k,l}(n)\left(\hat{s}_l^{(i)} - \bar{s}_l\right), & n < k \le N, \\ r_n - g_{n,n}(n)s_n - \sum_{l=n+1}^{N} g_{n,l}(n)\left(\hat{s}_l^{(i)} - \bar{s}_l\right), & k = n, \\ r_k - g_{k,n}(n)s_n - \sum_{l=k}^{n-1} g_{k,l}(n)\left(\hat{s}_l^{(i-1)} - \bar{s}_l\right) - \sum_{k=n+1}^{N} g_{k,l}(n)\left(\hat{s}_l^{(i)} - \bar{s}_l\right), & 1 \le k < n. \end{cases} \quad (22)$$

where $\sigma_k^2 = d_{k,k}^{-1}$, with $d_{k,k}$ being the mth diagonal element of the diagonal matrix $\mathbf{D}_n$, and the values of $\rho_{n,k}(s_n)$ is shown in (22). In (22), $g_{k,l}(n)$ is the element on the kth row and lth column of the equivalent channel matrix $\mathbf{G}_n$.

From (19) and (21), the APP of symbol s_n during the ith iteration can be calculated as

$$P\left(s_n^{(i)} = \chi_m|\mathbf{r}\right) = \prod_{k=1}^{N} \frac{1}{\pi\sigma_k} \exp\left\{-\frac{|\rho_{n,k}(\chi_m)|^2}{\sigma_k^2}\right\} \frac{P(s_n)}{p(\mathbf{r})}, \quad (23)$$

where $P(s_n)$ is the symbol *a priori* probability, and the value of $p(\mathbf{r})$ can be easily obtained by using the normalization $\sum_{m=1}^{M} P\left(s_n^{(i)} = \chi_m|\mathbf{r}\right) = 1$. The sequence-based symbol APP, $P\left(s_n^{(i)} = \chi_m|\mathbf{r}\right) = P\left(s_n^{(i)} = \chi_m|\mathbf{y}\right)$, is used to calculate the tentative soft decision as described in (9).

Eqn. (23) gives the APP for M-ary modulated symbol. To obtain the APP for binary code bit $x_{n,k}$, we define

$$\mathcal{S}_k^{(b)} \triangleq \{\chi_m|\chi_m \in \mathcal{S} : x_{n,k} = b\}, \text{ for } k = 0, \cdots, \log_2 M,$$

where $b \in \{-1, +1\}$, and $x_{n,k}$ is the kth bit of the binary vector $\mathbf{x}_n$ mapped to the symbol s_n. The APP of the bit $x_{n,k}$ in a system with M-ary modulation during the ith iteration can be expressed as

$$P\left(x_{n,k}^{(i)} = b|\mathbf{r}\right) = \sum_{s_n \in \mathcal{S}_k^{(b)}} p\left(\mathbf{r}|\mathbf{s}_n^{(i)}\right) P(s_n)/p(\mathbf{r}). \quad (24)$$

Combining (21) and (24) , we can write the LLR of the bit $x_{n,k}$ as

$$\Lambda\left(x_{n,k}^{(i)}|\mathbf{r}\right) = \ln \frac{\sum_{s_n \in \mathcal{S}_k^{(+1)}} \exp\left[-\sum_{j=1}^{n} \frac{1}{\sigma_j^2}|\rho_{n,j}(s_n)|^2\right] P(s_n)}{\sum_{s_n \in \mathcal{S}_k^{(-1)}} \exp\left[-\sum_{j=1}^{n} \frac{1}{\sigma_j^2}|\rho_{n,j}(s_n)|^2\right] P(s_n)}. \quad (25)$$

It should be noted that the terms, $\rho_{n,j}(s_n)$, for $j > n$, are independent of s_n, and they are canceled during the LLR evaluation.

The extrinsic information, $L_O(x_{n,k}^{(i)})$, which is the soft-output of the equalizer after the ith iteration, can then be calculated as

$$L_O(x_{n,k}^{(i)}) = \Lambda\left(x_{n,k}^{(i)}|\mathbf{r}\right) - L_I(x_{n,k}), \quad (26)$$

where $L_I(x_{n,k})$ is the *a priori* LLR for the ith iteration.

In the proposed algorithm, the soft-output is calculated by collecting information from the entire sample sequence, $\mathbf{r}$, as described in (22) and (25). The sequence-based equalization is enabled by tentative soft decisions from both previous iteration, $\hat{s}_n^{(i-1)}$, and the current iteration, $\hat{s}_n^{(i)}$. Errors usually exist in the tentative decisions, especially during the first few iterations. Inevitably, the performance of the algorithm will be negatively affected by error propagation, where an error in one tentative decision might lead to errors in subsequent decisions. The adopted soft decision will reduce the effects of error propagation, thus leads to better system performance. In addition, the number of errors in tentative decisions decreases with the increase of iterations, and this will reduce the performance gap between the proposed algorithm with its optimum counterpart.

C. A Simplified Algorithm

A simplified version of the SISO MMSE-BDFE algorithm is presented in this section to reduce the computational complexity of the proposed equalizer.

Compared to the classical symbol-based equalization methods, the proposed sequence-based detection incurs extra complexity during the calculation of the soft output. From (25), the calculation of each bit LLR requires the evaluation of nM metrics, $|\rho_{n,k}(s_n)|^2$, for $k = 1, \cdots, n$, and $s_n \in \mathcal{S}$, while only M metrics are required by symbol-based algorithms.

The complexity caused by sequence-based soft output calculation can be reduced by utilizing the structure of the equivalent channel matrix $\mathbf{G}_n$. The matrix $\mathbf{G}_n = \mathbf{U}_n$ is obtained from Cholesky decomposition, and the power of the matrix is concentrated on the elements that are close to its main diagonal. Fig. 3(a) showed the power distribution of the equivalent channel matrix $\mathbf{G}_n$ for a static channel with channel impulse response $\mathbf{h} = [0.227, 0.46, 0.688, 0.46, 0.227]$ [10]. In Fig. 3(a), the average power of the lth tap of the equivalent channel matrix is defined as

$$\bar{p}_l = \frac{1}{N-l} \sum_{k=1}^{N-l} |g_{k,k+l}|^2, \text{ for } l = 0, 1, \cdots, N-1. \quad (27)$$

It's apparent from the figure that, for the equivalent channel matrix $\mathbf{G}_n$, the power of the zero-th tap (main diagonal elements) is significantly larger than power of the remaining taps (off diagonal elements). In other words, the equivalent system is in its minimum phase state. Therefore, we can simplify the LLR calculation by discarding channel taps with negligible power without apparently affecting system performance.

The fifth iteration bit error rate (BER) of the above system at $E_b/N_0 = 11$ dB is shown in Fig. 3(b) as a function of the number of equivalent channel taps, J, used during detection. From Fig. 3(b), we have three observations. First, the proposed sequence-based detection ($J > 1$) outperforms classical symbol-based detection ($J = 1$). Second, for this example, no additional performance gain can be achieved when $J > 4$. Third, increasing J from 1 to 2 doesn't introduce apparent performance gain. This can be intuitively explained by the fact that the tentative soft decisions used by the second

channel tap has low qualities due to the negligence of the third and fourth channel taps.

Comparing the BER results in Fig. 3(b) with the channel tap power in Fig. 3(a), we conclude that neglecting equivalent channel taps with power at least 25 dB below the dominant tap power renders almost the same performance as considering all the channel taps. Thus the algorithm can be simplified by considering only dominant channel taps, without negatively affecting system performance. The complexities of the original method and simplified method are analyzed in the next subsection.

Another source of computational burden is from the evaluation of the MMSE-BDFE filters, which has similar complexities as the symbol-based methods. From (17), the formulation of each pair of $\mathbf{W}_n$ and $\mathbf{G}_n$ requires two matrix inversions and one Cholesky decomposition. Noting the fact that the calculation of the matrices, $\mathbf{W}_n$ and $\mathbf{G}_n$, requires only the second order *a priori* information, $\mathbf{\Phi}_n$, we can reduce the computational complexity by using a fixed covariance matrix for all symbols. If $\mathbf{\Phi} = \text{diag}[\sigma_{s_1}^2, \cdots, \sigma_{s_N}^2]$ is used for the formulation of $\mathbf{W}$ and $\mathbf{G}$, then only two matrix inversions and one Cholesky decomposition are needed for all the symbols within one block. From (18), we have an equivalent system with simplified calculations as

$$\mathbf{r}_n = \mathbf{W}[\mathbf{y} - \mathbf{H}\bar{\mathbf{s}}_n] = \mathbf{G}[\mathbf{s} - \bar{\mathbf{s}}_n] + \mathbf{e}. \tag{28}$$

In this simplified system representation, fixed matrices, $\mathbf{W}$ and $\mathbf{G}$, are used in combination with symbol dependent mean vectors, $\bar{\mathbf{s}}_n$. Analysis and simulation show that the performance loss due to replacing dynamic filters with fixed filters is negligible for practical system configurations. On the other hand, as shown in the next subsection, significant amount of computational efforts are saved by using fixed filters for all data symbols within one block.

D. Complexity Analysis

The computational complexity of the proposed SISO equalizer is analyzed and compared to that of linear MMSE algorithm. The complexity of the equalizer is mainly incurred by two sources: the sequence-based calculation of the soft output, and the formulation of the MMSE-BDFE filters.

From (22), the calculation of each metric, $|\rho_{n,k}(s_n)|^2$, requires $N - m + 2$ complex multiplications. The original sequence-based method requires nM such metrics for the evaluation of each bit LLR. Therefore, for a block with N data symbols, the number of complex multiplications required in one iteration is in the order of: $M \log_2 M \sum_{n=1}^{N} \sum_{m=1}^{n} (N - m + 2) + \mathcal{O}(1) = M \log_2 M \frac{N^3+3N^2+2N}{3} + \mathcal{O}(1) = \mathcal{O}(\frac{MN^3 \log_2 M}{3})$.

For the simplified algorithm, only JM metrics are required for each bit LLR, with $J << N$. Thus, the complexity of the simplified LLR calculation is reduced to the order of: $M \log_2 M \sum_{n=1}^{N} \sum_{m=n-J+1}^{n} (N - m + 1) + \mathcal{O}(1) = JM \log_2 M \frac{N^2+N(J+2)}{2} + \mathcal{O}(1) = \mathcal{O}(\frac{JMN^2 \log_2 M}{2})$.

From (17), the formulation of the full complexity MMSE-BDFE solution requires two matrix inversions and one Cholesky decomposition for each data symbol. The complexities of matrix inversion and Cholesky decomposition of a $N \times N$ matrix are in the order of $\mathcal{O}(N^3)$. Since there are N modulation symbols in each block, the computational effort required for the calculation of MMSE-BDFE filters is in the order of $N \times \mathcal{O}(N^3) = \mathcal{O}(N^4)$.

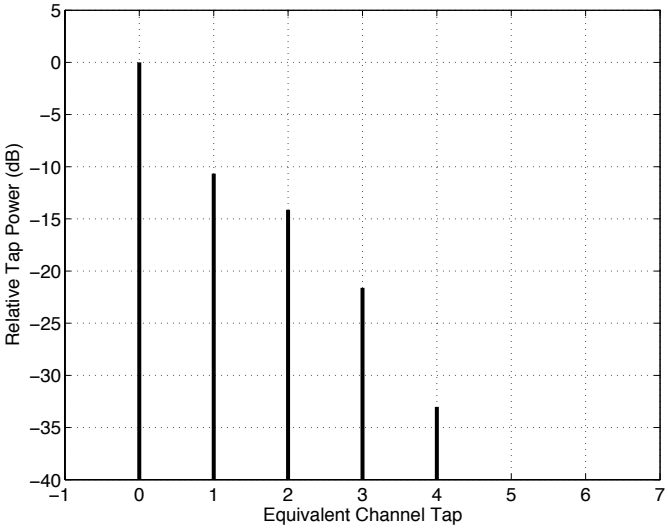

(a) Tap Power of Equivalent System

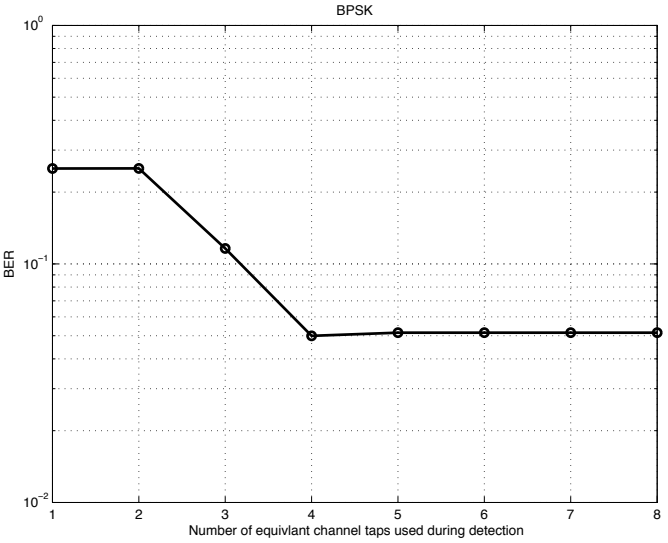

(b) BER v.s. Number of Taps used in Detection

Fig. 3. Impact of channel tap power on system performance.

The simplified algorithm uses fixed filters for all the symbols within one block. Thus the complexity incurred by MMSE-BDFE solution of the simplified version of the proposed algorithm is in the order of $\mathcal{O}(N^3)$.

Based on the analysis above, the full complexity turbo equalizer requires a computational complexity in the order of $\mathcal{O}\left(CN^4 + \frac{MN^3 \log_2 M}{3}\right)$, where C is a constant independent of M and N. Similarly, the complexity of the simplified algorithm is in the order of $\mathcal{O}\left(CN^3 + \frac{JN^2 \log_2 M}{2}\right)$.

Conventional symbol-based method, such as the MMSE algorithm proposed in [10], requires only M metrics for each bit LLR evaluation, thus has a complexity in the order of $\mathcal{O}(MN \log 2M)$ for soft output calculation. In addition, the formulation of the MMSE algorithm in [9] has a complexity of $\mathcal{O}(N^3)$ for a block of N symbols with the help of a fast

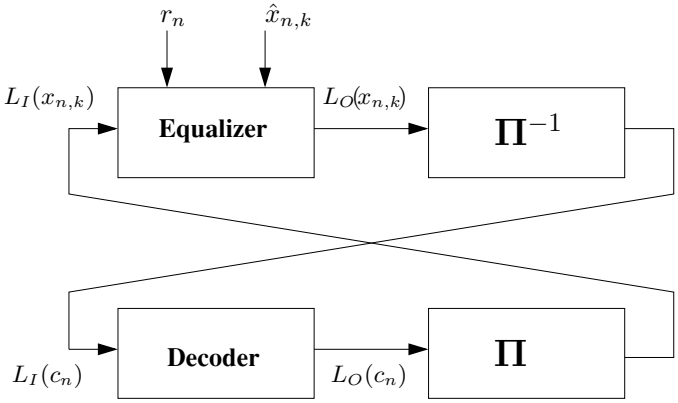

Fig. 4. Extrinsic information exchange of turbo equalization.

recursive matrix inversion method. Thus, the total complexity of MMSE algorithm has a complexity in the order of $\mathcal{O}\left(C'N^3 + \frac{MN\log_2 M}{2}\right)$, with C' being a constant.

From the analysis above, it is concluded that the linear MMSE algorithm in [9] has lower complexity compared to the full complexity proposed method, and has similar complexity as the simplified sequence-based equalizer. All of the suboptimum algorithms have less computational burden compared to trellis-based algorithms, whose complexity scales with M^{L-1}, with L being channel length.

IV. Performance Analysis with EXIT Chart

The performance of the proposed SISO equalizer is analyzed in this section by using the tool of extrinsic information transfer chart [19], which traces the evolution of mutual information between data symbols and its LLR through iterations.

The SISO equalizer/decoder can be modeled as a mutual information transfer device, *i.e.*, given *a priori* mutual information at the input, I_I, the equalizer/decoder generates a new mutual information, I_O, at the output by exploiting the channel/code structure. This concept is illustrated in Fig. 4. For a given input mutual information I_I, an output mutual information I_O at the output of the equalizer/decoder can be obtained by following the hybrid simulation and analytical method described in [10] or [19]. Thus, a mutual information transfer curve can be obtained for a given SISO equalizer or SISO decoder. By placing the mutual information transfer curves of equalizer and decoder in the same figure, the EXIT chart can illustrate the evolution of mutual information during various iterations of turbo equalization. Fig. 5 depicts the EXIT chart of several turbo equalizers with various SISO equalization algorithms and BCJR convolutional decoder. The horizontal axis represents the mutual information at the input of the equalizer, I_I^E, which is obtained from interleaving the output of the convolutional decoder, I_O^D. Similarly, the output of the equalizer, I_O^E, and the input of convolutional decoder, I_I^D, are represented on the vertical axis of the figure. The results obtained in Fig. 5 are obtained from the static channel described in Fig. 3. A convolutional code with rate $R = 1/2$ is used in the analysis. The generator polynomial of the convolutional code in octal notation is $G = [23, 35]_8$.

In the EXIT chart shown in Fig. 5, the iteration process between equalizer and decoder can be visualized by using

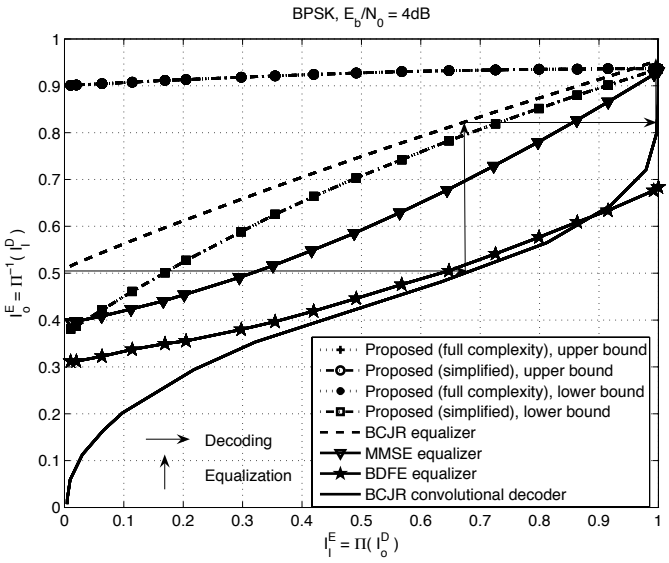

Fig. 5. EXIT charts of various SISO equalizers with BCJR convolutional decoder.

a trajectory trace following $I_O^E \rightarrow I_I^D$ and $I_O^D \rightarrow I_I^E$. The trajectory trace of the system with BCJR equalizer is drawn in the figure as an example. The vertical trace and horizontal trace represent the procedure of equalization and decoding, respectively. It can be seen from the figure that the mutual information improves by following the guide of the "tunnel" between the transfer curves of the equalizer and the decoder. The trajectory trace shows that the BCJR equalizer can converge in two iterations under the assumption of ideal interleaver and infinite block length. It might take more iterations to converge under practical system configuration.

As shown in Fig. 4, the proposed equalizer relies on both soft *a priori* input and soft decisions. Since the reliability of soft decisions changes with the evolution of iterations, the exact mutual information transfer curve of the proposed algorithm cannot be readily obtained with the method described in [19], which considers only soft *a priori* input. Therefore, the mutual information transfer curve of the proposed algorithm is illustrated under two extreme conditions: with perfect *a priori* soft decisions $\hat{x}_{n,k}^{(i-1)} = x_{n,k}$ (upper bound), and with zero *a priori* soft decision $\hat{x}_{n,k}^{(i-1)} = 0$ (lower bound). During the first iteration, where no *a priori* information is available, the system performance follows the lower bound; after several iterations, the *a priori* soft decisions become more reliable, and the upper bound gives a better indication of the mutual information transfer. The actual transfer curve of the proposed algorithm is in the middle between these two extreme conditions. Comparing the transfer curves of the proposed algorithm with other algorithms, we have the following observations.

First, the transfer curves of the simplified version of the proposed algorithm coincide with their full complexity counterparts. This indicates that the simplified algorithm has almost the same performance as the full complexity algorithm.

Second, the proposed algorithm converges faster than other algorithms. It can be seen from the trajectory trace that the convergence rate of iterative equalization is determined

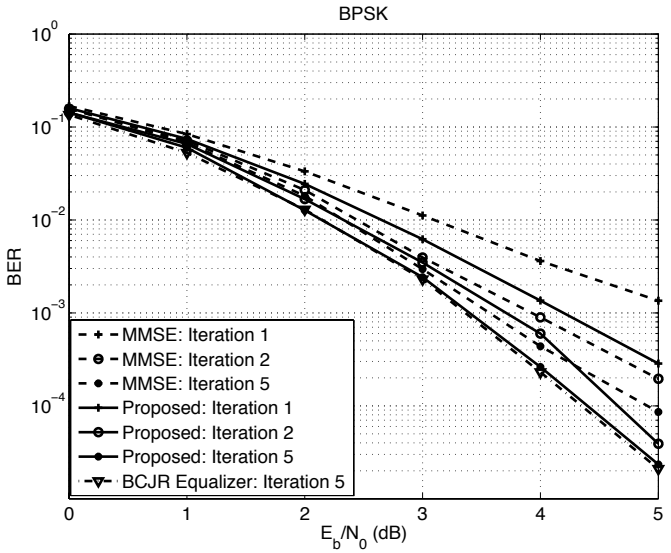

Fig. 6. BER performance of turbo equalization in BPSK system.

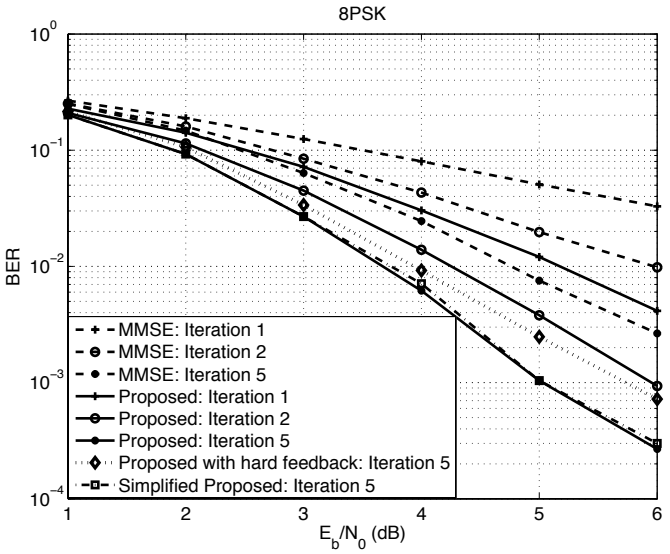

Fig. 7. BER performance of turbo equalization in 8PSK system.

by the width of the "tunnel" between equalizer curve and decoder curve. It's clear from the figure that the "tunnel" of the proposed algorithm is wider than other low complexity algorithms, therefore, it can reach its optimum performance point with fewer iterations. This will further reduce the overall computational complexity of turbo equalization.

Third, after convergence, the proposed algorithm and the linear MMSE algorithm [9] can achieve almost the same performance as the BCJR equalizer. However, the proposed algorithm can achieve the optimum performance with the least complexity due to its fast converging property.

V. Simulation Results

BER results obtained from simulations under practical system configurations are presented in this section to verify the performance of the proposed low complexity SISO MMSE-BDFE algorithm. The transmitted data is divided into blocks with length 2048-bit. One block is further cut into sub-blocks with length 128-bit. The SISO MIMO-BDFE is performed over sub-blocks, while BCJR convolutional decoding is performed over an entire block. Convolutional code with generator polynomial $G = [23, 57]_8$ is used in the simulation. To illustrate the performance of the system under practical system, the frequency selective fading is generated based on the Typical Urban profile [20]. The channel is constant within one block, and it varies from block to block. Each realization of the channel is normalized to unit energy.

Fig. 6 compares the performance of the proposed algorithm with that of the linear SISO MMSE algorithm in [9]. The simulation is performed for BPSK modulated systems. It's clear from the figure that the proposed non-linear MMSE-BDFE algorithm consistently outperforms the linear MMSE algorithm for all iterations. The performance gain is mainly contributed by the sub-optimum sequence-based detection. The BER obtained from the BCJR equalizer is also shown in this figure as a reference. During the fifth iteration, the performance of the proposed algorithm is almost the same as that of the BCJR equalizer. This result agrees with the analysis from EXIT chart. With the increase of iterations, the *a priori* soft decisions becomes more and more reliable, and this narrows down the performance gap between the proposed algorithm and trellis-based algorithm.

The performances of 8PSK modulated systems with various low complexity equalization algorithms are shown in Fig. 7. Again, the non-linear MMSE-BDFE algorithms outperforms the linear MMSE algorithm during the iterations considered. At the BER level of 3×10^{-3}, the fifth iteration performance of the MMSE-BDFE algorithm is 1.3 dB better than that of the MMSE algorithm. In addition, the proposed algorithm converges faster than the linear MMSE algorithm: the second iteration performance of the proposed algorithm is better than the fifth iteration performance of the MMSE algorithm. Based on the EXIT chart analysis, the MMSE algorithm can eventually achieve the same performance as the proposed algorithm, but with much more iterations. To illustrate the impact of soft decision, the fifth iteration BER performance of the proposed algorithm with hard decision feedback is also shown in the figure. At the BER level of 10^{-3}, using hard decision feedback results in a performance loss of 0.8 dB.

The performance of the simplified MMSE-BDFE algorithm with fixed filters and time varying mean vectors is also shown in this figure. From the figure, the simplified version of the proposed algorithm has almost the same performance as the full complexity MMSE-BDFE algorithm. As analyzed in Section III-D, the simplified algorithm has similar complexity as the linear MMSE algorithm. Thus, the proposed simplified non-linear equalizer can achiever better performance with similar complexity as the linear MMSE algorithm.

VI. Conclusions

A low complexity SISO MMSE-BDFE algorithm for turbo equalization was presented in this paper. With the help of both soft *a priori* information and soft decision of the data symbols, the output of the equalizer is obtained by evaluating an approximation of the sequence-based APP of the data symbols. The accuracy of the APP approximation obtained

in the proposed algorithm improves with the evolution of iterations, and this reduces the performance gap between the proposed algorithm and trellis-based algorithms. Performance analysis revealed that the performance improvement of the proposed algorithm over linear MMSE algorithm is achieved at the cost of complexity. To reduce the computational complexity, a simplified version of the SISO MMSE-BDFE was presented. The simplified algorithm has similar complexity as linear MMSE algorithm, and it can achieve a performance similar to that of trellis-based algorithms.

ACKNOWLEDGMENTS

The authors are grateful to the anonymous reviewers and the Editor, Dr. John R. Barry, for their careful reviews and valuable comments that have helped us improve the quality of the paper.

REFERENCES

[1] C. Douillard, M. Jezequel, C. Berrou, A. Picart, P. Didier, and A. Glavieux, "Iterative correction of intersymbol interference: turbo-equalization," *Euro Trans. Telecommun.*, vol.6, no.5, pp.507-511, Sept.-Oct. 1995.

[2] C. Berrou, A. Glavieux, and P. Thitimajshima, "Near Shannon limit error-correcting and decoding: turbo codes (1)," in *Proc. IEEE Int. Conf. Commun.*, vol.2, May, 1993, pp.1064-1070.

[3] L.R. Bahl, J. Cocke, F. Jelinek, and J. Raviv, "Optimal decoding of linear codes for minimizing symbol error rate," *IEEE Trans. Inform. Theory*, vol. IT-20, pp.284-287, Mar. 1974.

[4] J. Hagenauer, "A Viterbi algorithm with soft-decision outputs and its application," in *Proc. IEEE GLOBECOM '89*, pp.1680-1686, Nov. 1989.

[5] J. Park and S. B. Gelfand, "Sparse MAP equalizers for turbo equalizations", in *Proc. IEEE VTC'05-Spring*, pp. 762-766, June 2005.

[6] J. Moon and F. R. Rad, "Turbo equalization via constrained-delay APP estimation with decision feedback", *IEEE Trans. Commun.*, vol. 53, no. 12, pp. 2102–2113, Dec. 2005.

[7] X. Wang and H.V. Poor, "Iterative (turbo) soft interference cancellation and decoding for coded CDMA," *IEEE Trans. Commun.*, vol.47, pp.1046-1061, July 1999.

[8] A. Dejonghe and L. Vandendorpe, "Turbo-equalization for multilevel modulation: an efficient low complexity scheme," in *Proc. IEEE Int. Conf. Commun.*, pp. 1863-1867, May 2002.

[9] M. Tuchler, A.C. Singer, and R. Koetter, "Minimum mean square error equalization using a priori information," *IEEE Trans. Signal Processing*, vol.50, pp. 673–683, Mar. 2002.

[10] M. Tuchler, R. Koetter and A.C. Singer, "Turbo equalization: principles and new results," *IEEE Trans. Commun.*, vol.50, pp.754-767, May 2002.

[11] S. Jiang, L. Ping, H. Sun, and C. S. Leung, "Modified LMMSE turbo Equalization", *IEEE Commun. Lett.*, vol. 8, no. 3, pp. 174–176, Mar. 2004.

[12] L. Liu and L. Ping, "An extending window MMSE turbo equalization algorithm", *IEEE Signal Processing Lett.*, vol.11, pp.891-894, Nov. 2004.

[13] S.L. Ariyavisitakul and Y. Li, "Joint coding and decision feedback equalization for broadband wireless channels," *IEEE J. Select. Areas Commun.*, vol.16, pp.1670-1678, Dec. 1998.

[14] Z. -N. Wu and J. M. Cioffi, "Low-complexity iterative decoding with decision-aided equalization for magnetic recording channels", *IEEE J. Selected Areas Commun.*, vol. 19, no. 4, pp. 699–708, Apr. 2001.

[15] R. R. Lopes and J. R. Barry, "The soft-feedback equalizer for turbo equalization of highly dispersive channels," *IEEE Trans. Commun.*, vol.54, pp.783-788, May 2006.

[16] A. Stamoulis, and G.B. Giannakis, and A. Scaglione, "Block FIR decision-feedback equalizers for filterbank precoded transmissions with blind channel estimation capabilities," *IEEE Trans. Commun.*, vol.49, pp.69-83, Jan. 2001.

[17] C. Xiao, J. Wu, S.Y. Leong, Y.R. Zheng, and K.B. Letaief, "A discrete-time model for triply selective MIMO Rayleigh fading channels," *IEEE Trans. Wireless Commun.*, vol.3, pp.1678-1688, Sept. 2004.

[18] S. -J. Lee, A. C. Singer, and N. R. Shanbhag, "Linear turbo equalization analysis via BER transfer and EXIT Charts", *IEEE Trans. Signal Processing*, vol. 53, pp. 2883–2897, Aug. 2005.

[19] S. ten Brink, "Designing iterative decoding schemes with the extrinsic information transfer chart", *AEU Int. J. Electron. Commun.*, vol. 54, pp. 389–398, Nov. 2000.

[20] ETSI. GSM 05.05, "Radio transmission and reception," ETSI EN 300 910 V8.5.1, Nov. 2000.

Jingxian Wu (S'02-M'06) received the B.S. (EE) degree from the Beijing University of Aeronautics and Astronautics, Beijing, China, in 1998, the M.S. (EE) degree from Tsinghua University, Beijing, China, in 2001, and the Ph.D. (EE) degree from the University of Missouri at Columbia, MO, USA, in 2005.

Dr. Wu is an Assistant Professor at the Department of Engineering Science, Sonoma State University, Rohnert Park, CA, USA. His research interests mainly focus on the physical layer of wireless communication systems, including multicarrier communications, space-time coding, channel estimation and equalization, and spread spectrum communications.

Dr. Wu is currently an Associate Editor for the IEEE TRANSACTIONS ON VEHICULAR TECHNOLOGY. Since 2006, he has served as a Technical Program Committee member for a number of international conferences, including the IEEE Global Telecommunications Conference, the IEEE Wireless Communications and Networking Conference, and the IEEE International Conference on Communications. Dr. Wu is a member of Tau Beta Pi.

Yahong Rosa Zheng (S'99-M'03-SM'07) received the B.S. degree from the University of Electronic Science and Technology of China, Chengdu, China, in 1987, the M.S. degree from Tsinghua University, Beijing, China, in 1989, both in electrical engineering. She received the Ph.D. degree from the Department of Systems and Computer Engineering, Carleton University, Ottawa, ON, Canada, in 2002.

From 1989 to 1997, she held Engineer positions in several companies. From 2003 to 2005, she was a Natural Science and Engineering Research Council of Canada (NSERC) Postdoctoral Fellow at the University of Missouri, Columbia, MO, USA. Since fall 2005, she has been an Assistant Professor with the Department of Electrical and Computer Engineering at the Missouri University of Science and Technology (former University of Missouri-Rolla), Rolla, MO. Her research interests include array signal processing, wireless communications, and wireless sensor networks.

Dr. Zheng is currently an Associate Editor for the IEEE TRANSACTIONS ON WIRELESS COMMUNICATIONS. She has served as a Technical Program Committee member for the IEEE International Sensors Conference 2004, the IEEE Global Telecommunications Conference 2005 — 2007, the IEEE International Conference on Communications 2006 — 2008, and the IEEE Wireless Communications Networking Conference 2008. She has also served as technical reviewer for many international and IEEE journals.